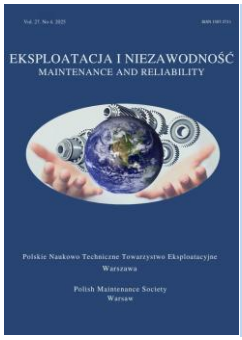

Eksploatacja i Niezawodnosc – Maintenance and Reliability
Volume 27 (2025), Issue 4
journal homepage: http://www.ein.org.pl

Article citation info:
Zhuang Y, Gu Y, Yan M, Mou C, Jin Y, Huang Z, Ren Y, Research and Reliability Analysis on the Impact of Biomimetic Groove Group Arrangement Structures on the Sealing Performance of Sealing Rings, Eksploatacja i Niezawodnosc – Maintenance and Reliability 2025: 27(4) http://doi.org/10.17531/ein/203544

Research and Reliability Analysis on the Impact of Biomimetic Groove Group Arrangement Structures on the Sealing Performance of Sealing Rings

Indexed by:
Web of Science Group

Yuhao Zhuang[a], Yunqing Gu[a,*], Muhan Yan[a], Chengqi Mou[b], Yuxin Jin[a], Zhangcheng Huang[a], Yun Ren[c]

[a] College of Metrology Measurement and Instrument, China Jiliang University, Hangzhou 310018, China.
[b] College of Energy Engineering, Zhejiang University, Hangzhou 310027, China
[c] Zhijiang College, Zhejiang University of Technology, Shaoxing 312030, China

Highlights

- The exploration and analysis of the reliability of sealing performance of biomimetic non-smooth surface structures applied to sealing rings.
- A comparative study of biomimetic grooved seal rings and smooth surface seal rings.
- A comparative study on the internal flow field of centrifugal pumps with sealing rings of different biomimetic arrangement structures.

Abstract

By analyzing the surface structures of biological organisms and extracting various biomimetic circular groove non-smooth surface structures, the sealing ring in the centrifugal pump is used as a carrier to explore the reliability of the application of biomimetic non-smooth surface structures in sealing performance. A computational model is established to numerically simulate centrifugal pumps equipped with different biomimetic circular groove structures for sealing rings. By comparing and analyzing the pump characteristic curves, internal flow fields, and leakage characteristics of biomimetic circular groove structures with different groove group arrangements, it was found that overly complex biomimetic circular groove arrangements have a negative impact on the enhancement of sealing performance. Further research was conducted on the influence of different biomimetic groove group arrangement radii on sealing performance. The study found that when the groove group radius is 1°, the changes in the head and efficiency of the centrifugal pump are relatively minor. At this time, the centrifugal pump with a biomimetic circular groove structure sealing ring applied under this circular groove structure can achieve the minimum leakage and maximum volumetric efficiency, demonstrating good sealing performance. This provides a theoretical basis for the reliability of applying biomimetic non-smooth surface structures in the sealing field.

Keywords
reliability, biomimetic non-smooth surface, groove array structure, sealing ring, sealing performance

1. Introduction

Biomimetics, also known as bionics, biomimetic engineering, or bio-mimetic technology, involves observing, learning from, and imitating nature to apply biological structures, functions, mechanisms, and behaviors to modern technology, thereby promoting technological progress and innovation [1]. Biomimetic non-smooth surfaces are a hot topic in the fields of materials science and engineering, aiming to create artificial materials with excellent functions by imitating the surface

(*) Corresponding author.
E-mail addresses: Y. Zhuang 948533977@qq.com, Y. Gu (ORCID: 0000-0003-4036-3140) guyunqing@cjlu.edu.cn, M. Yan s20020804068@cjlu.edu.cn, C. Mou 12127107@zju.edu.cn, Y. Jin 2301400206@cjlu.edu.cn, Z. Huang 2301400308@cjlu.edu.cn, Y. Ren renyun@zzjc.edu.cn

structures and characteristics of organisms in nature [2]. The surfaces of many organisms in nature exhibit unique microstructures, which not only endow them with specific physical and chemical properties but also provide important design inspiration for scientific research. Many organisms have surface designs with excellent fluid control characteristics. As early as 2005, Ren [3] et al. proposed the application of biomimetic non-smooth surfaces in mechanical sealing technology. Current biomimetic mechanical sealing technology mainly relies on changing surface shapes, creating various forms of grooves or micro-holes on sealing end faces to improve the lubrication between end faces. The design of biological surface structures not only reduces friction but also slows down or controls the occurrence of cavitation [4-6] through surface textures, maintaining stable sealing performance over long-term use [7].

To date, the grooves researched domestically and internationally on mechanical sealing end faces mainly include circumferential grooves [8], straight chord grooves [9], triangular grooves, semicircular grooves, rectangular grooves [10], arc-shaped grooves, leaf-shaped grooves, spiral grooves [11], herringbone grooves, and T-shaped grooves. Among these, spiral grooves are the most widely applied and researched, and they or their combinations are most commonly used. Traces of biomimicry can be found in various groove shapes. Researchers have discovered non-smooth surface groove structures on some organisms in nature, such as the dorsal fin of the suckerfish [12], which has evolved over time to form a shape resembling a sucker [13]. The adhesion force of the abalone's foot [14] is composed of vacuum adhesion, van der waals forces, and capillary forces, effectively enhancing adhesion [15]. Additionally, the surface unit distribution of shells is generally grooved, with groove spacing below 50 μm, and the ridges are nearly equal or radially symmetrical. Studies have shown that these grooves can reduce resistance and have good wear resistance. The microstructure of the lotus leaf surface [16] possesses superhydrophobicity, effectively preventing water adhesion and keeping the surface dry [17]. This self-cleaning characteristic can be applied to fluid mechanical seals. By mimicking its surface structure, researchers have successfully developed sealing materials with similar functions. The technology of end-face grooved mechanical seals is essentially a biomimetic non-smooth surface technology. Moreover, the design concept of biomimetic non-smooth surfaces can also be used to enhance the wear resistance of sealing materials. Many biological surfaces have self-healing abilities, for example, the shells of certain snails [18] can gradually recover their original shape when worn. This characteristic is particularly important in fluid mechanical seals because seals often face harsh conditions such as friction [19] and wear. By introducing biomimetic designs, researchers have been able to develop more wear-resistant sealing materials [20], extending the service life of equipment.

The main focus of this paper is the reliability of the sealing effect of bionic sealing rings [21], that is, the study of the clearance of bionic sealing rings. A sealing ring is usually installed at the inlet of the pump impeller to prevent the liquid in the pump from leaking. However, during the operation of the pump, due to the influence of physical properties, a pressure difference will occur between the two sides of the sealing ring, with the pressures on the two sides being close to the impeller outlet pressure and the impeller inlet pressure, respectively. Therefore, some liquid will leak from the side near the impeller outlet to the side near the impeller inlet. Although these leaking liquids also obtain energy from the impeller, they cannot be discharged from the impeller outlet, thereby reducing the water supply of the pump. According to the law of conservation of energy, the energy of the leaking liquid will be entirely used to overcome the resistance of the sealing ring, thus increasing the energy consumption of the pump.

Wang [22] et al. has found through research that the diameter of the sealing ring has a significant impact on the change in pressure difference between the two sides. The larger the diameter of the sealing ring, the greater the pressure difference between the two sides, and the more liquid will leak. The size data of commonly used pumps have already been determined. To reduce the amount of leaking liquid and thereby improve the efficiency of the pump, the clearance of the sealing ring is reduced within the allowable range. Under normal circumstances, the clearance of the sealing ring in a centrifugal pump is approximately chosen to be 0.002 times the diameter of the sealing ring. When assembling the sealing ring into the pump body, it is necessary to avoid excessive eccentricity of the sealing ring, as excessive eccentricity will also increase the

leakage [23]. To maintain a small leakage rate for non-contact impeller sealing rings, it is necessary to generate higher flow resistance, which is due to the nature of non-contact sealing. In other words, the use of non-contact sealing between the pump and the impeller sealing ring means that a certain amount of flow performance must be sacrificed to ensure sealing quality.The clearance seal of the impeller sealing ring is the most common form in centrifugal pumps. The overall performance of centrifugal pumps, as well as axial and radial forces, are all affected by the clearance and structure of the sealing ring. This is because they directly influence the volumetric losses and internal flow conditions of the pump. Enhancing the sealing performance of the sealing ring is of great significance for improving the efficiency of fluid machinery and ensuring stability and safety during operation.

To investigate the impact of the arrangement structure of biomimetic groove groups on the reliability of sealing performance of sealing rings, a centrifugal pump sealing ring was used as a carrier, and the sealing ring was treated with biomimetic non-smooth processing. A bionic circular groove structure based on the epidermal groove structure of chinese loach was designed on the surface of the seal ring, and numerical simulation was conducted on it. Based on this biomimetic circular groove structure, the arrangement of the grooves was altered, and numerical simulation was used to explore the strength of the sealing performance of the centrifugal pump under different arrangement structures. By analyzing the performance of the sealing rings with different arrangements and comparing their sealing effects, the strong sealing mechanism of the biomimetic circular groove structure was demonstrated, providing a theoretical basis for the application of biomimetic non-smooth structures in the field of sealing performance.

2. Characteristics of the body surface of the chinese loach and model establishment

2.1. Characterisation of the surface of the chinese loach

The chinese sucker loach is a species of fish that lives in the rapid waters of mountain streams, with a small body size, usually having smooth scales and a slender body. To overcome the impact of water currents, it has evolved a special abdominal tissue that uses the sealed environment formed between the tissue and the stone wall. Due to the sealing performance of the tissue, the inside of its abdomen does not exchange with the external environment, allowing it to firmly adhere to the stone wall. The stone walls of mountain streams are quite different from ordinary rocks; due to the scouring of water currents, the stone walls in the streams are smooth on the surface, similar to the smooth surface of centrifugal pump impellers. Therefore, applying biomimicry to sealing rings is possible. Research on the chinese sucker loach has revealed that it has distinct groove structures on its dorsal and caudal fins. At the tail and the posterior part of the abdomen, it is clear to observe the crossing and overlapping of the left and right posterior fins, with approximately 2-4 fin rays on each side. In addition, each posterior fin ray has 15-25 nodular units with a size of about 200 μm. Upon further magnification of the chinese sucker loach's posterior fin, as shown in figure 1, it can be observed that the fin rays are densely covered with hair-like bodies, with the diameter of the bodies gradually increasing from bottom to top. From figure 1 (a), small nodular units can be seen section by section, and the mound structure on the posterior fins of the chinese sucker loach and the small nodular units covering the fins form a multistage structure, which can be utilised to keep them firmly attached to the rock wall.

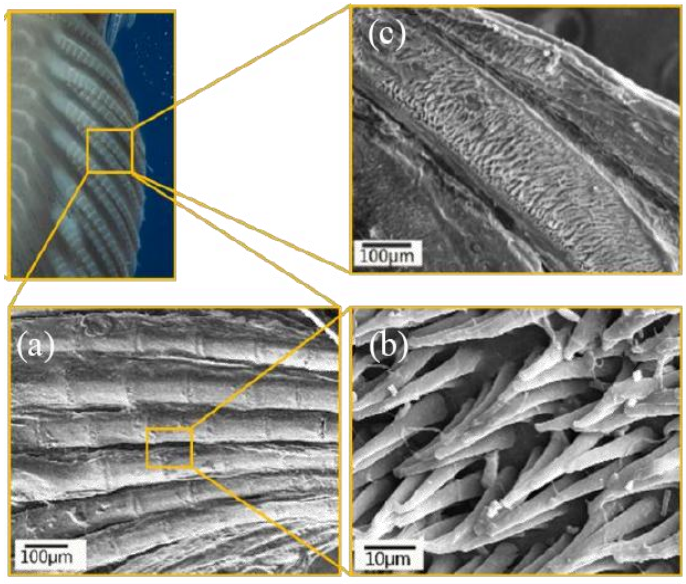

Figure 1. Schematic diagram of the groove structure on the body surface of the chinese sucker loach [24].

2.2. Model establishment

Select the IS 125-100-250 centrifugal pump as the carrier for applying biomimetic non-smooth surface treatment on its

sealing ring.

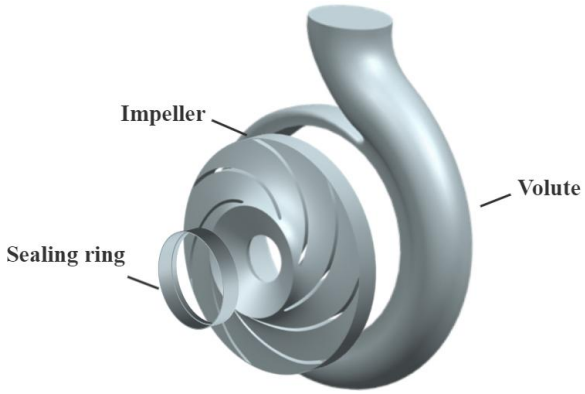

Figure 2. The main components model of a centrifugal pump.

The centrifugal pump model consists of six parts: the suction pipe, discharge pipe, impeller, volute casing, front cover plate and sealing ring, as shown in figure 2. The pump's inlet diameter is 125 mm, and the outlet diameter is 272 mm. The performance parameters of the centrifugal pump are a flow rate of 175 m^3/h, head of 21.6 m, power of 11.97 kw, efficiency of 84.94%, and rotational speed of 1480 r/min.

The modeling of the sealing ring draws on the structure of the grooves on the body surface of the chinese sucker loach and the arrangement of dermal grooves on the tiger shark's skin [25]. By analyzing these structures and combining the characteristics of circular groove structures with those of shield scale structures, a circular groove structure based on the shield scale arrangement was designed and applied to the sealing ring. As shown in the figure 3, it is a schematic diagram of the circular groove structure. Based on the circular groove structure, the original groove arrangement was altered, and elements of shield scales were incorporated to design a simpler shield scale circular groove structure. For ease of calculation, a sealing ring with a gap of 0.2 mm was selected, with the groove depth set to l=0.1 mm, the groove spacing to d=1 mm, and the radian between groove groups to 10°.

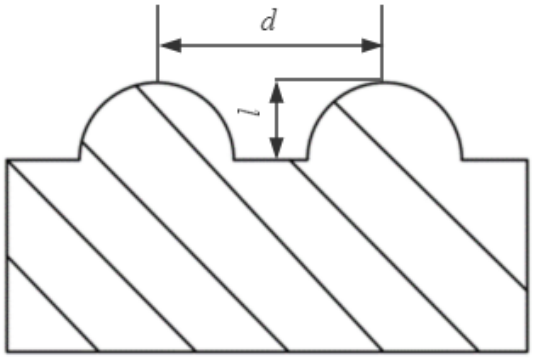

(a) Schematic diagram of the circular groove structure

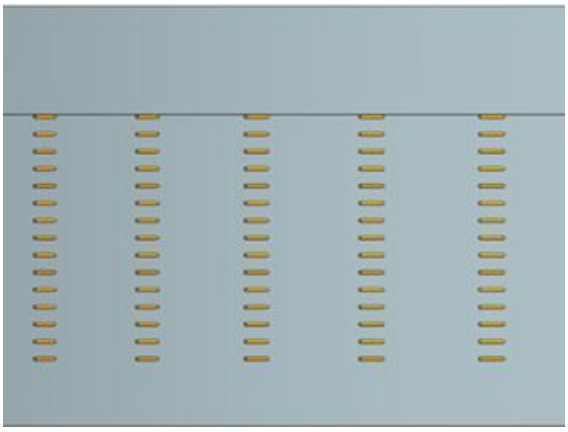

(b) Schematic diagram of the groove structure model

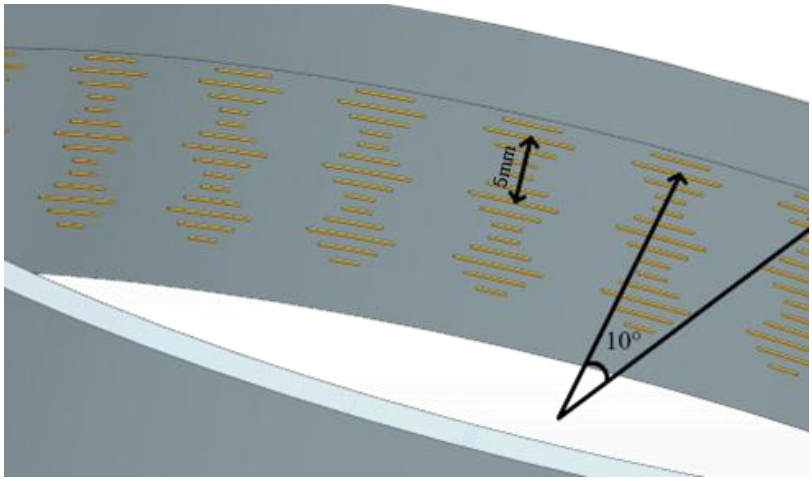

(c) Circular groove sealing ring designed based on the shield scale

Figure 3. Schematic diagram of the sealing ring model structure.

3. Numerical calculation methods

In numerical simulation, the finite volume element analysis method is used, with clear water as the fluid medium. Due to the complexity of the flow field inside the centrifugal pump, the standard *k-ε* model and the Realizable *k-ε* model are commonly used. Considering that the simulation requires separated flow calculations with complex secondary flows [26,27], the Realizable *k-ε* model can more accurately predict the development of turbulence, capture smaller-scale vortex structures , and respond more accurately to flows in shear layers. Therefore, the realizable *k-ε* model is adopted in the research process.

The realizable *k-ε* model [28] can be expressed as:

$$\begin{cases} \dfrac{\partial k}{\partial t}+\dfrac{\partial k u_j}{\partial x_j}=\dfrac{\partial}{\partial x_j}\left(Dk_{\text{eff}}\dfrac{\partial k}{\partial x_j}\right)+G_{\text{k}}-\varepsilon \\ \dfrac{\partial \varepsilon}{\partial t}+\dfrac{\partial \varepsilon u_j}{\partial x_j}=\dfrac{\partial}{\partial x_j}\left(D\varepsilon_{\text{eff}}\dfrac{\partial \varepsilon}{\partial x_j}\right)+\sqrt{2}C_{1\varepsilon}S_{ij}\varepsilon-C_{2\varepsilon}\dfrac{\varepsilon^2}{k+\sqrt{v\varepsilon}} \end{cases} \tag{1}$$

In the equation, k is the turbulent kinetic energy, ε is the turbulent dissipation rate. S_{ij} represents the average strain rate. The dimensionless number x_j represents Cartesian coordinates, u_j is the velocity component, t is the computational time. $C_{1\varepsilon}$ and $C_{2\varepsilon}$ are set as constants. G_k represents the generation of turbulent kinetic energy due to the mean velocity gradient, and Dk_{eff} and $D\varepsilon_{\text{eff}}$ are the effective diffusion rates of k and ε, respectively.

$$Dk_{\text{eff}}=v+v_{\text{t}} \tag{2}$$

$$D\varepsilon_{\text{eff}}=v+\frac{v_{\text{t}}}{\sigma_{\varepsilon}} \tag{3}$$

In the equation, σ_{ε} is the turbulent Planck number for ε, v is the turbulent viscosity, $v_t=C_{\mu}k^2/\varepsilon$, set C_{μ} as a constant.

Meshing is performed using ANSYS Fluent Meshing, and by refining the grid in the fluid domain, the head and efficiency of five experimental groups with different grid quantities are obtained. The figure 4 shows the mesh diagram of the sealing ring.

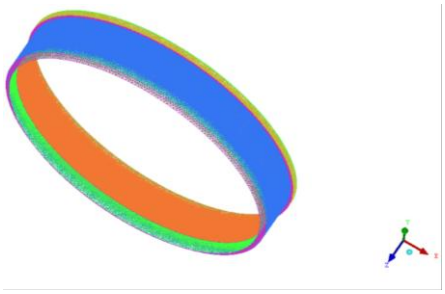

(a) Seal ring mesh diagram

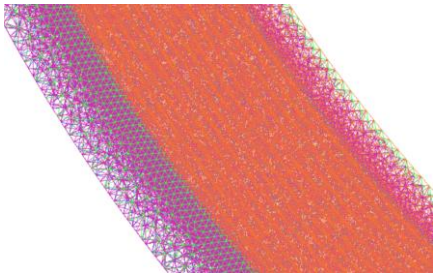

(b) Sealing ring gap grid

Figure 4. Mesh Generation

During the simulation process, when the number of grids exceeds 1.69 million, the change in head and efficiency tends to stabilize. This indicates that the head and efficiency results from the numerical simulation are less sensitive to the number of grids and remain basically stable. Therefore, 1.69 million grids are selected as the optimal configuration for the study. Current simulations typically only consider the effects of major components such as the impeller, sealing ring, volute and front cover plate, while ignoring the potential impacts of other complex flow factors. As a result, the pump head, efficiency and other external characteristic data obtained from numerical simulations may deviate from the actual situation in practical applications. The temperature of the fresh water used in the numerical simulation is maintained at 25℃ and standard atmospheric pressure is selected as the external pressure.

4. The impact of the arrangement of circular groove structures on sealing performance

4.1. The impact of different arrangements of circular groove structures on sealing performance

Figure 5 shows the hydrostatic pressure distribution of the seal ring with different structures on the z=0 datum plane. Figure 5 (c) changes the arrangement of the circular groove structure and applies the arrangement of the shield scale structure in order to investigate whether the different arrangements have any effect on the internal flow field. Comparing the three different sealing ring structures, it can be found that the gradient of the internal flow field distribution [29] is consistent, which indicates that the pressure field distribution law of the centrifugal pump with the shield-scaled circular groove surface structure sealing ring

is consistent with the nature of the centrifugal pump. Comparing the three structures horizontally, the pressure distribution part of the contact area between the impeller and the seal ring has a big difference, the leakage at the untreated seal ring is bigger, which makes the leakage generate more pressure, so the pressure on the smooth surface marked in the figure is bigger than that of the two different arrangements of the circular groove structure. However, for the sealing ring with the shield scale groove surface structure, the pressure is higher than the initial circular groove surface structure, and it can be found that the shield scale groove surface structure performs better compared to the smooth surface, but is weaker than the original circular groove structure. The effect of the complexity of the bionic groove structure on the performance of the microdevice is obvious, if the bionic structure is too complex, it will cause turbulence in the internal flow field.

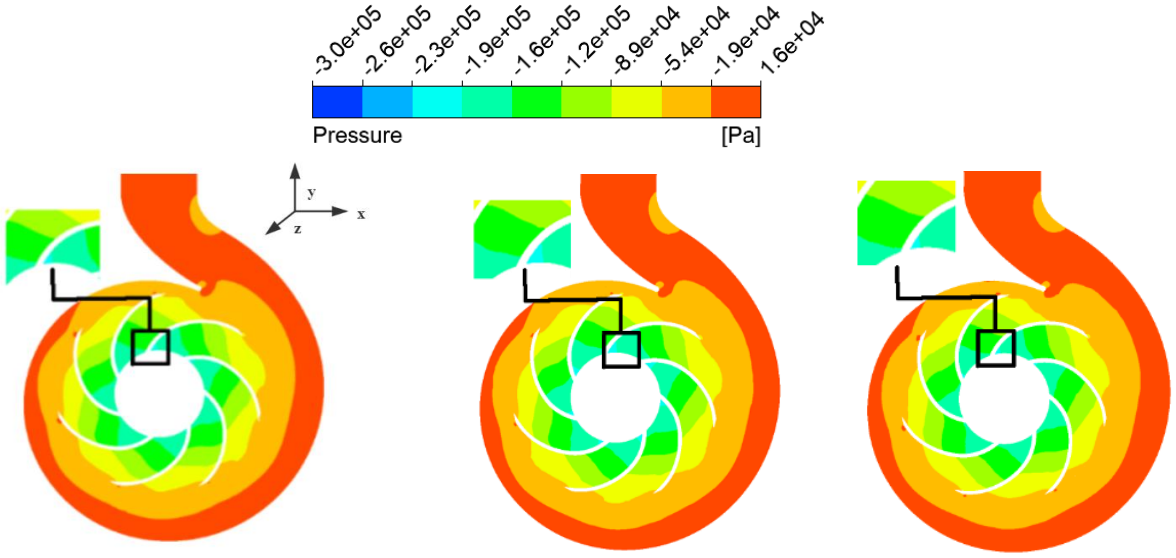

(a) Smooth surface structure (b) Circular groove structure (c) Shield scale groove structure

Figure 5. Static pressure distribution on the z=0 reference plane under different structural sealing rings.

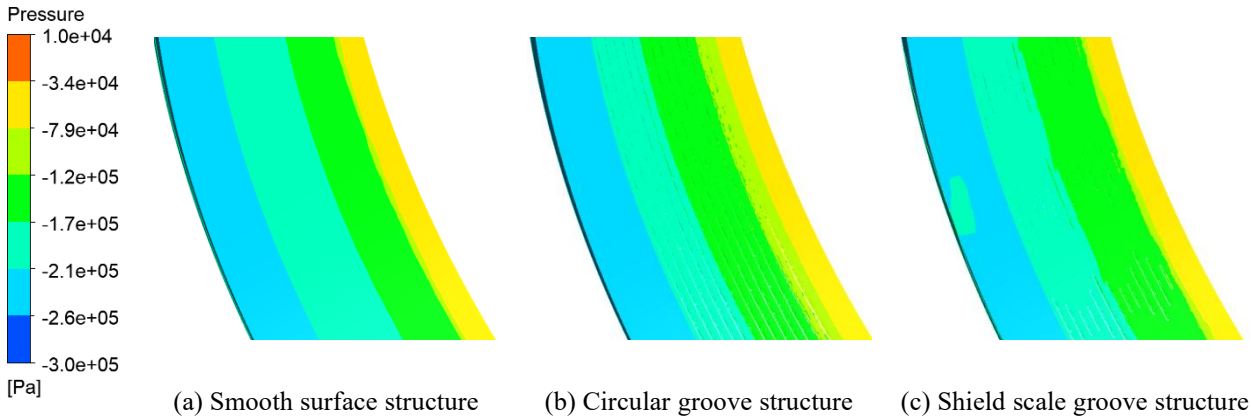

(a) Smooth surface structure (b) Circular groove structure (c) Shield scale groove structure

Figure 6. Static pressure distribution diagram of sealing rings with different structures.

As shown in figure 6 (a) the pressure distribution on the seal ring of the smooth surface structure is very uniform, and the overall presentation of the pressure from the inlet end to the outlet end is from large to small, and the pressure distribution of the seal ring of the circular groove structure in figure 6 (b) is more uniform, basically the same as the smooth surface structure, and there is no major impact, however, observing figure 6 (c) can be found that there is a relatively high pressure in the low-pressure area of the seal ring of the shield scale type circular groove structure.However there is also relative high pressure in the low pressure region, and the overall boundary fluctuation is large, which has a certain effect on the external characteristics of the centrifugal pump.

Based on the above analysis applied to the surface of the bionic groove structure can not be made too complex, the flow in the seal ring is too complex, will cause the flow of the flow channel flow in the flow of violent collision, resulting in flow energy loss, resulting in the seal ring gap in the flow field

disorder. Although the bionic groove structure with uneven curvature can improve the sealing performance of the sealing ring, this type of structure, such as the arrangement of the shield scale structure, will also reduce the overall efficiency of the centrifugal pump, and will not be able to achieve the optimal effect.

4.2. Design of the sealing ring structure with circular groove groups

The biomimetic circular groove structure with uneven arrangement radian may suppress the sealing effect of the sealing ring. Therefore, a circular groove structure imitating the chinese sucker loach is adopted, and the radian of the groove groups is fine-tuned to improve sealing performance. The impact of circular groove structures with different groove group radian β (as shown in figure 7 and figure 8) on the sealing performance of the centrifugal pump is studied, and four sealing rings are designed while keeping their structure relatively simple.

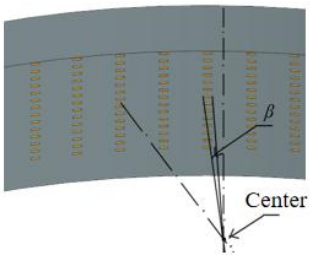

Figure 7. Schematic diagram of the sealing ring with a circular groove surface structure featuring a groove group with a radius of β

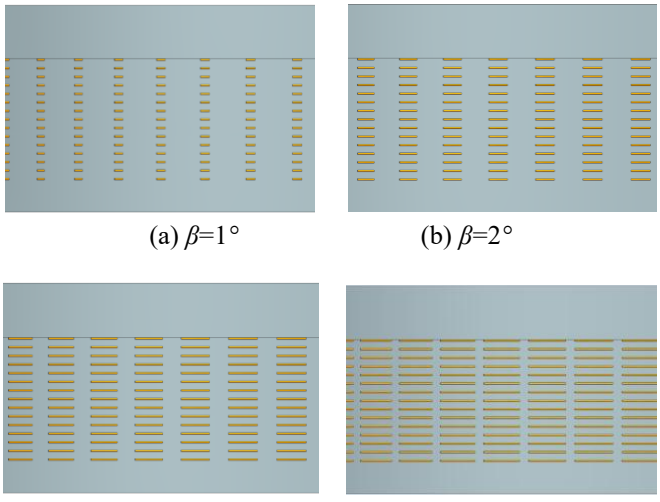

(a) β=1° (b) β=2°

(c) β=3° (d) β=4°

Figure 8. Sealing rings with circular groove surface structures of different groove group radian β.

4.3. Analysis of the external characteristics of pumps with circular groove group structure sealing rings

Figure 9 is a bar chart of the external characteristics of centrifugal pumps with sealing rings of different circular groove group radian. The original circular groove surface structure is used as the control group, in other words, the groove group at an interval of 0°. As shown in figure 9 (a), the head of the centrifugal pump with five different circular groove group radian sealing rings has a certain relationship with the radian, the head generally increases with the increase in radian, reaching the maximum head when the radian is at its maximum of 360°. Since the centrifugal pump operates through the rotation of the impeller, the rotation of the impeller drives the fluid, giving the fluid kinetic energy, which is then converted into pressure energy and finally reflected in the head. Therefore, if the leakage is large, the head is small, indirectly indicating weak sealing performance; conversely, a large head indicates strong sealing performance. By comparing the heads of centrifugal pumps with different arcs of circular groove groups, it can be found that the head is the smallest when the arc is 2°, and the head is the largest when the arc is 4°, without considering the control group. The larger the arc of the groove group, the fewer the number of circular grooves arranged in the same column, so that the distribution of circular groove structure increases, when the arc is 4°, without considering the control group, the number of circular grooves is the least, the distribution of its sealing ring is the most, the formation of the dense circular grooves will form a vortex, which will make it difficult for the fluid from the sealing ring to escape from the outlet end of the ring, when the arc of 2°, the number of circular grooves and distribution is relatively small, at this time, the vortex is the largest. When the arc is 2°, the number and distribution of circular grooves is relatively small, the number of vortices is small, the distribution of vortices in the internal flow field is more unconcentrated, and the consumption of the fluid to obtain kinetic energy is greater. Which compares β=1°, at this time the sealing ring although it does not look as dense as β=2°, but β=1° when the overall area of the grooves is still greater than the area of β=2°, so β=2° head is less than β=1° head, so in general, the head will increase with the increase of the curvature. The difference in head between the five structures is not very large, so the effect of this can be almost ignored.

Due to the non-significant changes in head, further research is conducted from the aspect of efficiency. Figure 9 (b) shows the bar chart of the efficiency of centrifugal pumps with sealing rings of different circular groove group radian. Observations from the chart reveal that the efficiency of centrifugal pumps with five different circular groove group radian sealing rings changes with the radian in a trend nearly consistent with the change in head; as the radian of the groove group increase, the efficiency of the centrifugal pump also increases. Excluding the control group, when the radian is 4°, the centrifugal pump has the highest head and also the highest efficiency. Overall, the difference in head among centrifugal pumps with different sealing ring structures is not very large, and the difference in efficiency is relatively small as well. Even when the radian is 1°, the efficiency of the centrifugal pump with the circular groove structure sealing ring decreases by 0.232% compared to the efficiency when the radian is 4°, but when precision is set to one decimal place, the difference is actually quite minor. When the differences in head and efficiency are not significant, further research is continued into the relationship between leakage and volumetric efficiency and the change in radian. Figures 9 (c) and (d) represent the leakage and volumetric efficiency of sealing rings with different groove group radian, respectively. Comparing the leakage, it is found that when the radian is 1°, the leakage is the smallest among the five structures, while the volumetric efficiency [30] is the largest, indicating that the sealing performance is the strongest among the four circular groove structures.

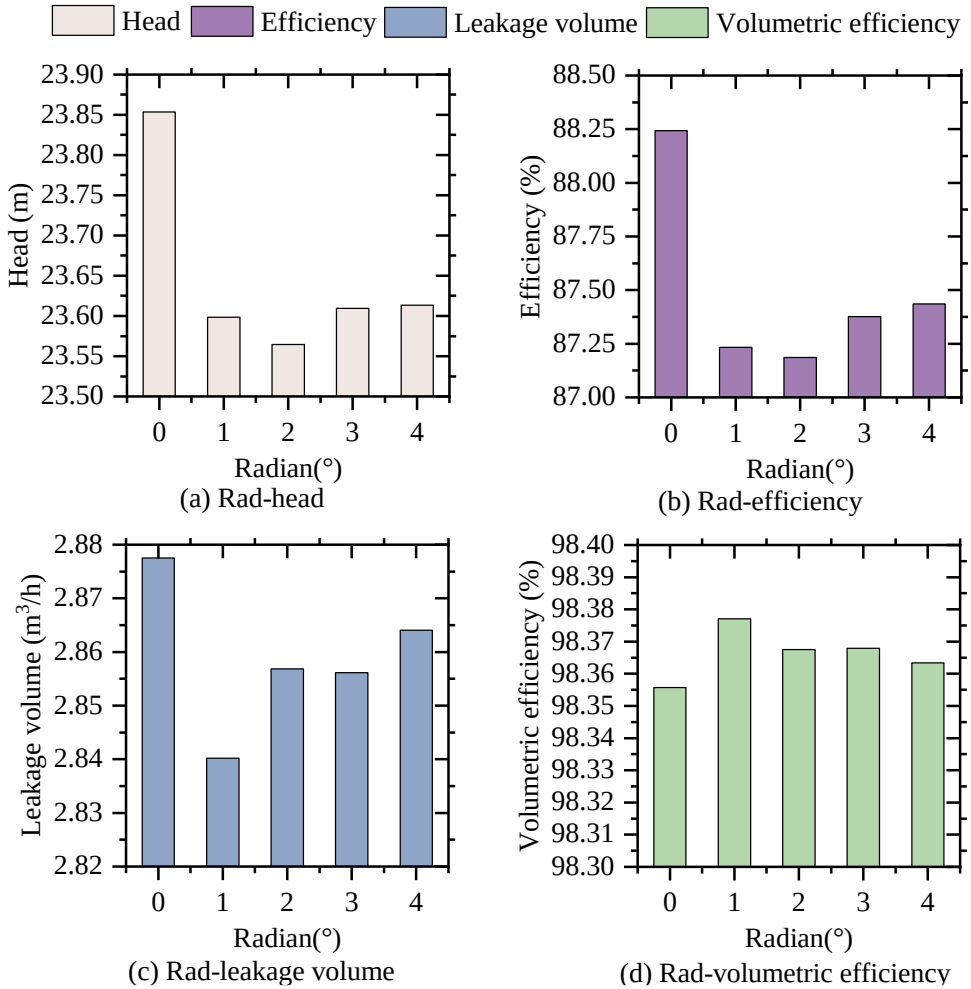

Figure 9. Bar chart of the external characteristics of centrifugal pumps with sealing rings of different circular groove group radian β.

From figure 9, it can be seen that the external characteristic indices of the centrifugal pump have a certain relationship with the radian of the groove groups. As the radian of the groove groups increase, the arrangement of the circular groove surface structure has a certain impact on the head, efficiency, and other external characteristics of the centrifugal pump. The circular groove surface structure causes changes in the structure of the sealing ring surface, and the walls in contact with the volute casing and impeller are altered differently. The fluid forms vortices between the grooves, these vortices lead to a certain

consumption of kinetic energy. Under the combined influence of the number and distribution of the groove groups, the formation of vortices requires a certain amount of kinetic energy conversion, resulting in a reduction of energy in the main stream of fluid ejected from the volute casing, causing a certain energy loss. Therefore, the external characteristics such as head and efficiency are less than those of the control group. If biomimetic groove structures are applied to actual working conditions and operations, they can enhance the sealing performance of the centrifugal pump without affecting its normal operation and use.

4.4. Analysis of the internal flow field of pumps with circular groove group structure sealing rings

Figure 10 is a schematic diagram of the impeller sealing ring and figure 11 shows the gap pressure contour of sealing rings with circular groove surface structures at different groove group radian β. By examining the relationship between the sealing rings with different groove group radian β and the internal flow field, the relationship between sealing performance and the groove group radian β is revealed. From the figure, it can be observed that the high-pressure area at the outlet end of the sealing gap gradually shifts towards the middle section. The pressure at the inlet end of the sealing gap remains nearly consistent among the five structures, indicating that the stability of the four structures can be ensured. As the fluid gains energy from the rotation of the impeller and is then ejected through the volute casing, the pressure is highest at the outlet end of the sealing gap. The increase in the high-pressure area in the middle section is due to the enhancement of sealing performance, which leads to an increase in flow rate at the outlet end, demonstrating a positive correlation between pressure and flow rate. When the groove group radian β increases from 1° to 4°, the pressure change from the inlet end of the sealing gap to the front section of the middle section is almost zero, while the pressure change from the middle section to the outlet end is still quite significant. The results indicate that when β=1°, the sealing performance of the sealing ring is relatively the best, with a more uniform pressure distribution.

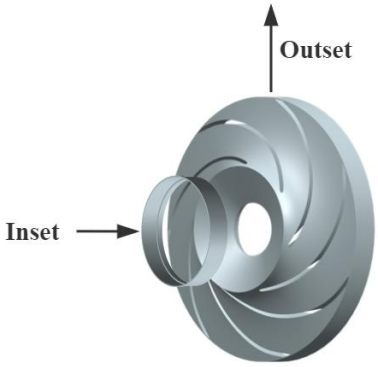

Figure 10. Impeller sealing ring schematic diagram.

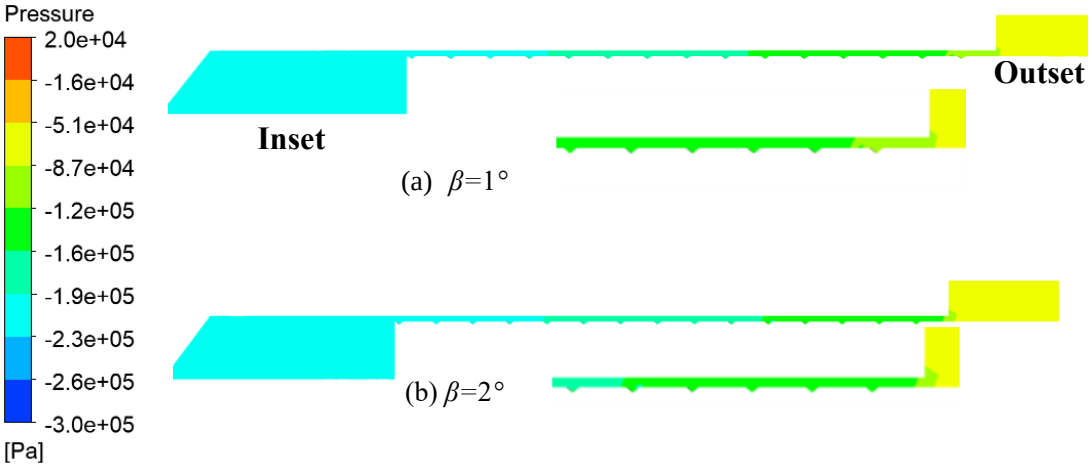

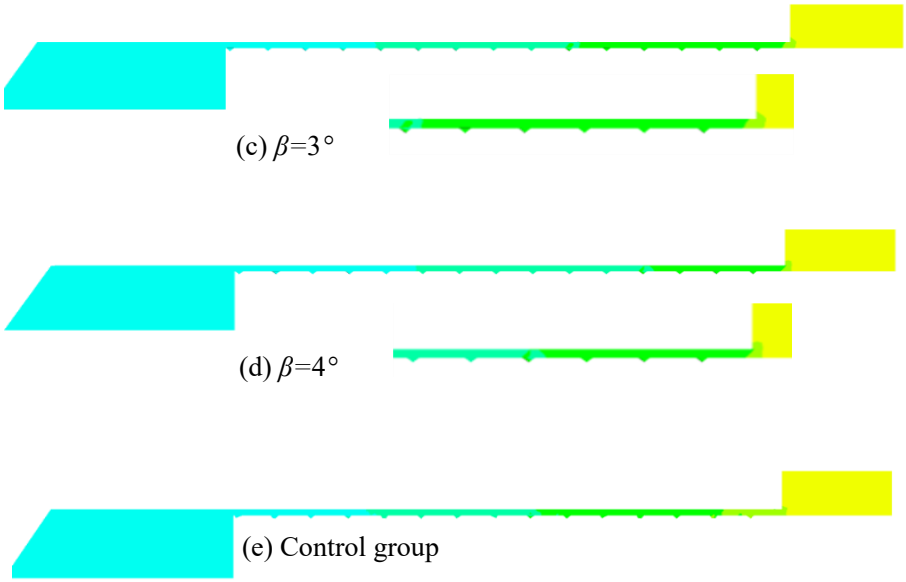

Figure 11. Gap pressure contour of sealing rings with groove structures at different radian β.

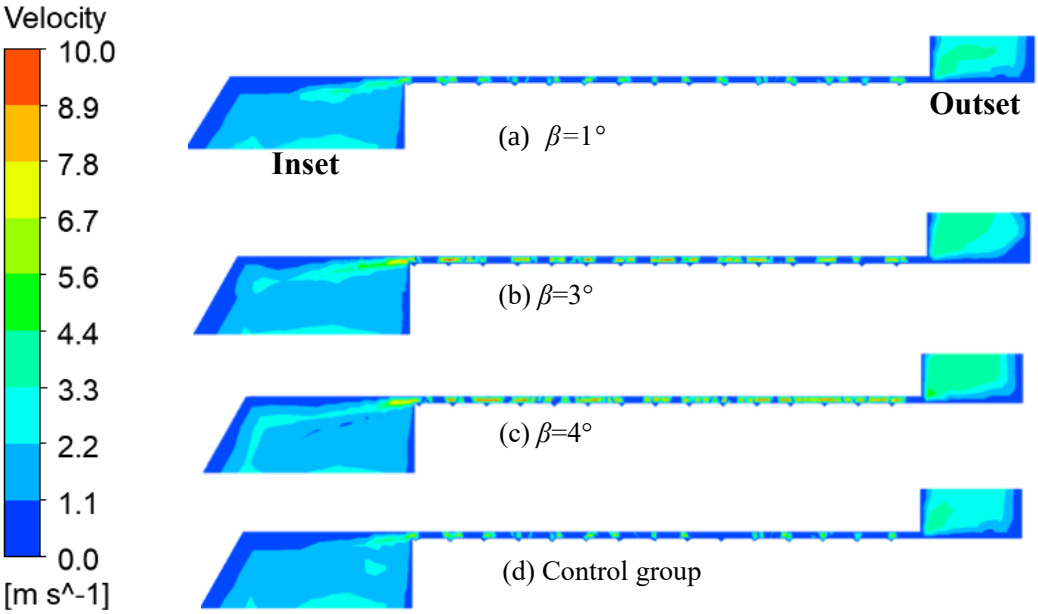

Figure 12. Gap velocity contour of sealing rings with groove structures at different radian β.

Figure 12 shows the gap velocity contour of sealing rings with circular groove surface structures at different groove group radian β. By observing the gap pressure contours of sealing rings with groove structures at different radian β, it can be seen that when β=1°, excluding the control group, the sealing performance of the sealing ring is the best at this time. The inlet end of the gap velocity cloud diagram for the five structures gradually decreases as the radius decreases. It is evident that when β=2°, there is a strong velocity disturbance from the inlet end to the middle section and then to the outlet end of the sealing gap, which is due to the relatively weak sealing performance. As a result, the fluid can flow through the inlet end of the sealing gap, through the middle section, to the outlet end of the sealing gap. Similar to the changes at the inlet end, as the radius β gradually increases, the velocity in the middle section of the sealing gap gradually decreases. When β=1°, the velocity distribution is essentially consistent with the control group, and the distribution of high and low velocities also shows similar changes. There is a high concentration of high-velocity distributions in the grooves of the sealing gap, with high-velocity fluids primarily located at the bottom of the sealing ring's groove structure. This is because when the fluid flows to the grooves, vortices are formed, and the formation of these vortices accelerates the fluid.

Figure 13 shows the vorticity distribution of the sealing ring under different groove group radian. It can be seen from the

figure that the overall vorticity distribution on the sealing ring increases with the increase in groove group radian[31]. Comparing each vorticity diagram, it is evident that when the circular groove group radius β is 1°, most of the vorticity is concentrated in the circular groove groups, while only a small amount of vorticity exists on the smooth surfaces between the groove groups. However, as the radius of the circular groove groups increases, the vorticity on the smooth surfaces between the groove groups gradually increases. When the circular groove groups are absent and only a complete circular groove remains, as in the control group, the vorticity is uniformly distributed across the entire surface of the sealing ring. Since all models are hydraulic models, the groove structure is raised in the hydraulic model, while in the solid model, the groove structure is recessed. Logically, if the groove structure is closer to the impeller wall, then the smooth surface should have more vorticity distribution than the circular groove surface, which is contrary to what is shown in the figure. This is because the presence of the circular groove structure creates a weak vacuum state between the grooves, making it difficult for the fluid to flow from the smooth surface structure. Therefore, this verifies the above conclusion that the sealing performance is strongest at this time.

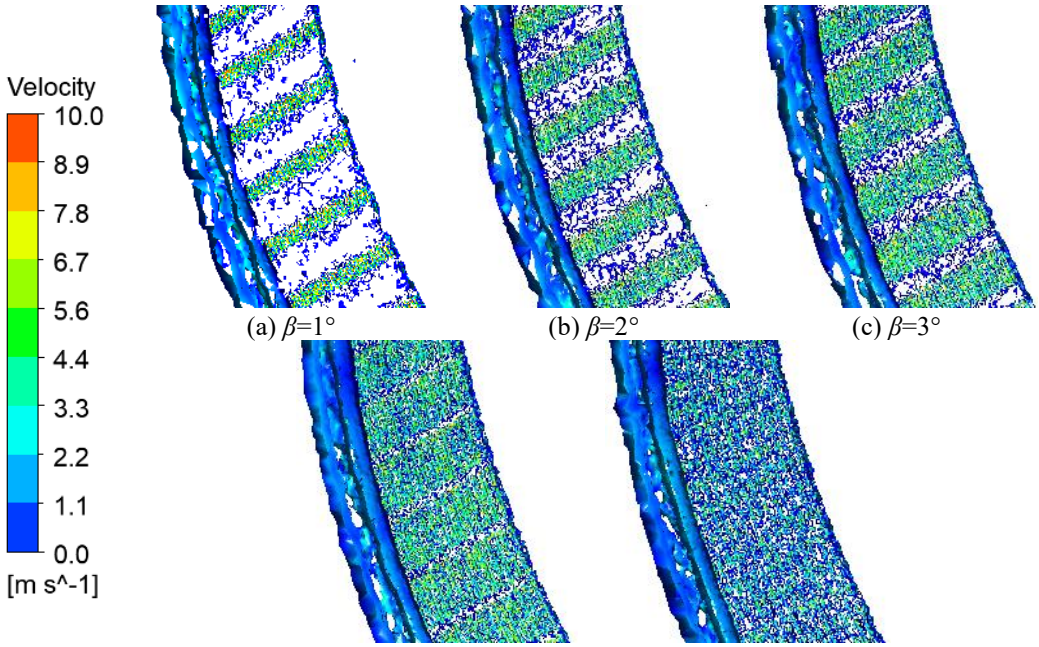

(a) β=1° (b) β=2° (c) β=3°

(d) β=4° (e) Control group

Figure 13. Vorticity diagrams of sealing rings at different groove group radian β.

5. Conclusion

(1) Based on the biological characteristics of the chinese sucker loach, a circular groove structure mimicking the skin structure of the chinese sucker loach was proposed for application on the sealing ring of centrifugal pumps to enhance sealing performance. The impact on the internal flow field distribution and external characteristics of the centrifugal pump was studied through numerical simulation, and a computational model of the biomimetic groove surface sealing ring was established, the exploration and analysis of the reliability of applying biomimetic non-smooth surface structures in the sealing field have been conducted.

(2) Sealing rings with different arrangement structures have a certain impact on the internal flow field distribution of the centrifugal pump. The array of circular groove surface structures with a shield scale structure can form vortices that interact with each other, reducing the efficiency of the centrifugal pump. The sealing ring with a neatly arranged circular groove structure has the best sealing performance, different arrangement structures are key factors affecting the reliability of sealing performance for sealing rings applied with biomimetic non-smooth surfaces.

(3) Through research and comparative analysis, it was found that the circular groove surface structure at a groove group radius of 1° exhibited relatively minor changes in head and efficiency. At this time, the centrifugal pump with the circular groove surface structure sealing ring demonstrated the smallest

leakage and maximum volumetric efficiency under this structure. This verified that the biomimetic groove structure has good sealing effects.

(4) The sealing mechanism of the biomimetic non-smooth surface structure is reflected in: the non-smooth surface structure increases the contact area with the sealing material, and the presence of groove structures creates a weak vacuum state between the grooves, making it difficult for the fluid to flow from the smooth surface structure parts, preventing the fluid from easily flowing out of the outlet end of the sealing ring, thus achieving a sealing effect, provide a theoretical basis for the reliability of applying biomimetic non-smooth surface structures in the sealing field.

This study systematically investigated the reliability of the application effects of biomimetic non-smooth surface structures in the sealing rings of centrifugal pumps through numerical simulation and theoretical analysis. The results indicate that optimizing the arrangement and design of the groove structures can significantly enhance sealing performance. However, there are certain limitations to this study: firstly, the results obtained from numerical simulation need to be further validated through experiments; secondly, the study mainly focuses on the application in centrifugal pumps, and the applicability to other types of pumps or fluid machinery requires further exploration. Future research plans include conducting experimental validation and exploring the potential applications of biomimetic non-smooth surface structures in a broader range of fluid machinery.

Funding

This study was supported by the Fundamental Research Funds for the Provincial Universities of Zhejiang (2023YW88), and the Zhejiang Provincial Natural Science Foundation of China (No. LY22E050015).

References

1. Barthlott W, Rafiqpoor M D, Erdelen W R. Bionics and biodiversity-bio-inspired technical innovation for a sustainable future. SFB-TRR 141 Public Conference on Biological Design and Integrative Structures - Analysis, Simulation and Implementation in Architecture, Stuttgart, Germany. Biomimetic Research for Architecture and Building Construction: Biological Design and Integrative Structures 2016; 9: 11-55, DOI:10.1007/978-3-319-46374-2_3.
2. Wang D F, Chen D D, Chen Z Y. Recent progress in 3D printing of bioinspired structures. Frontiers in Materials 2023; 7: 286, DOI:10.3389/fmats.2020.00286.
3. Ren L Q, Yang Z J, Han Z W. Non-smooth wearable surfaces of living creatures and their bionic application. Transactions of the Chinese Society for Agricultural Machinery 2005; 36(7): 144-147.
4. Gu Y Q, Qiu Q F, Ren Y, Ma L B, Ding H X, Hu C X, Wu D H, Mou J G. Cavitation flow of hydrofoil surface and turbulence model applicability analysis. International Journal of Mechanical Sciences 2024; 277: 109515, DOI:10.1016/j.ijmecsci.2024.109515.
5. Qiu Q F, Gu Y Q, Ma L B, Hu C X, Ding H X, Wu D H, Mou J G, Wu Z X. Study of non-constant local cavitation suppression in micro-wedge structure. Physics of Fluids 2024; 36(1): 015150, DOI:10.1063/5.0191165.
6. Gu Y Q, Yin Z F, Yu S W, He C D, Wang W T, Zhang J J, Wu D H, Mou J G, Ren Y. Suppression of unsteady partial cavitation by a bionic jet. International Journal of Multiphase Flow 2023; 164: 104466, DOI:10.1016/j.ijmultiphaseflow.2023.104466.
7. Zhang X, Jiang J B, Peng X D, Ni Z J. Experimental and numerical simulation study on the influence of structural factors on the leakage characteristics of clearance seals. Flow Measurement and Instrumentation 2023; 94: 102465, DOI:10.1016/j.flowmeasinst.2023.102465.
8. Zhang H G, Aa K, Wu Y H, Chu W L, Tan F. Mechanism of affecting ability of casing treatment to improve stall margin with varying axial position of circumferential grooves. Journal of Propulsion Technology 2016; 37(12): 2296-2302, DOI:10.13675/j.cnki.tjjs.2016.12.012.
9. Zhou G W, Mi X W, Wang J X, Hu R K. Experimental comparison between the Stribeck curves of water lubricated rubber bearing with straight and spiral grooves. Industrial Lubrication and Tribology 2018; 70(7): 1326-1330, DOI:10.1108/ILT-10-2017-0296.
10. Zhang S D. Effect of groove structure on lubrication performance of water-lubricated stern tube bearings. Lubricants 2023;11(9): 374, DOI:10.3390/lubricants11090374.
11. He T, Zhang Q Q, Yan Y, Dong J T, Zhou P. Numerical simulation of a new designed mechanical seals with spiral groove structures. Lubricants 2023; 11(2): 70, DOI:10.3390/lubricants11020070.
12. Wang S Q, Li L, Sun W G, Wainwright D, Wang H, Zhao W, Chen B H, Chen Y F, Wen L. Detachment of the remora suckerfish disc:

kinematics and a bio-inspired robotic model. Bioinspiration & Biomimetics 2020, 15(5), 056018, DOI:10.1088/1748-3190/ab9418.

13. Cohen K E , Tobalske B W, Crandell K E and Shadwick R E. Sucker with a fat lip: the soft tissues underlying the viscoelastic grip of remora adhesion. Journal of Anatomy. 2020; 237(4): 643-654, DOI:10.1111/joa.13227
14. Xi P, Cong Q, Xu J, Sun L. Surface movement mechanism of abalone and underwater adsorbability of its abdominal foot. Bioinspired Biomimetic and Nanobiomaterials 2019; 8(4): 1800044, DOI:10.1680/jbibn.18.00044.
15. Xi P, Ye S B, Cong Q. Abalone adhesion: the role of various adhesion forces and their proportion to total adhesion force. PLOS One 2023; 18(6): e0286567, DOI:10.1371/journal.pone.0286567.
16. Koch K, Bhushan B, Barthlott W. Multifunctional surface structures of plants: an inspiration for biomimetics. Progress in Materials Science 2009; 54(2): 137-178, DOI:10.1016/j.pmatsci.2008.07.003.
17. Solga A, Cerman Z, Striffle B F, Spaeth M, Barthlott W. The dream of staying clean: Lotus and biomimetic surfaces. Bioinspiration & Biomimetics 2007; 2(4): S126, DOI:10.1088/1748-3182/2/4/s02.
18. Cremaldi J C, Bhushan B. Bioinspired self-healing materials: lessons from nature. Beilstein Journal of Nanotechnology 2018; 9: 907- 935, DOI:10.3762/bjnano.9.85.
19. Gu Y Q, Ma L B, Yan M H, He C D, Zhang J J, Mou J G, Wu D H, Ren Y. Strategies for improving friction behavior based on carbon nanotube additive materials. Tribology International 2022; 176: 107875, DOI:10.1016/j.triboint.2022.108165.
20. Hao M M, Zhou R, Sun P T, Wang Z M, Ma T, Ren B J. Experimental study on friction characteristics of contact mechanical seal in start-up and stop stages. Lubrication Engineering 2023; 48(9): 41-46, DOI:10.3969/j.issn.0254-0150.2023.09.005.
21. Yan N, Wang X H, Wu X D, Zhu J W. Study on the form of sealing ring and its sealing characteristics of centrifugal pump. 4th IAHR Asian Working Group Symposium on Hydraulic Machinery and Systems, Kashgar, China. Journal of Physics: Conference Series 2024, 2752(1): 012117, DOI:10.1088/1742-6596/2752/1/012117.
22. Wang Y, Zhang X. Effect of clearance of impeller wear-rings on efficiency of low specific speed centrifugal pump. Drainage and Irrigation Machinery 2008; 26(6): 27-30.
23. Wang Y. Study on the leakage loss of volume of the wear-ring of the centrifugal pump. Hangzhou: Zhejiang University of Technology 2015.
24. Fan J X. The adhesion structure of sinogastromyzon and its high-performance adhesion mechanism. Changchun: Jilin University 2020.
25. Qin L G, Sun H J, Yang H, Zeng Q F, Dong G N. Numerical simulation on drag reduction performance of shark skin with denticle structures. China Sciencepaper 2019; 14(12): 1271-1277. DOI: 10.3969/j.issn.2095-2783.2019.12.001
26. Barrio R, Fernández J, Blanco E, Parrondo J. Estimation of radial load in centrifugal pumps using computational fluid dynamics. European Journal of Mechanics-B/Fluids 2011; 30(3): 316-324, DOI: 10.1016/j.euromechflu.2011.01.002.
27. Song X G, Park J H, Kim S G, Park Y C. Performance comparison and erosion prediction of jet pumps by using a numerical method. Mathematical and Computer Modelling 2013; 57(1-2): 245-253, DOI: 10.1016/j.mcm.2011.06.040.
28. Shaheed R, Mohammadian A, Gildeh H K. A comparison of standard k-ε and realizable k-ε turbulence models in curved and confluent channels. Environmental Fluid Mechanics 2019, 19(2): 543-568, DOI:10.1007/s10652-018-9637-1.
29. Jia X Q, Zhang Y, Lv H, Zhu Z C. Study on external performance and internal flow characteristics in a centrifugal pump under different degrees of cavitation. Physics of Fluids 2023; 35(1): 014104, DOI:10.1063/5.0133377.
30. Stawiński Ł, Kosucki A, Cebulak M, Górski A G V, Grala M. Investigation of the influence of hydraulic oil temperature on the variable-speed pump performance. Eksploatacja i Niezawodność - Maintenance and Reliability 2022; 24(2): 289-296. DOI:10.17531/ein.2022.2.10.
31. Chew J W, Gao F, Palermo D M. Flow mechanisms in axial turbine rim sealing. Proceedings of the Institution of Mechanical Engineers, Part C: Journal of Mechanical Engineering Science 2019; 233(23-24): 7637-7657, DOI:10.1177/0954406218784612.